

An Optimal Multiline TRL Calibration Algorithm*

Dylan F. Williams¹, C. M. Wang¹, and Uwe Arz²

¹National Institute of Standards and Technology, 325 Broadway, Boulder, CO 80305

²Physikalisch-Technische Bundesanstalt, Bundesallee 100, 38116 Braunschweig, Germany

Abstract — We examine the performance of two on-wafer multiline Thru-Reflect-Line (TRL) calibration algorithms: the popular multiline TRL algorithm implemented in the MultiCal[®] software package, and a newly implemented iterative algorithm designed to give optimal results in the presence of measurement noise. We show that the iterative algorithm outperforms the MultiCal software in the presence of measurement noise, and verify its uncertainty estimates.

I. INTRODUCTION

We compare the multiline Thru-Reflect-Line (TRL) vector-network-analyzer calibration algorithm of [1] implemented in the MultiCal[®] software package³ to a multiline TRL calibration algorithm based on the less-well-known iterative approach of [2]. We show that the iterative approach of de-embedding on-wafer scattering-parameter measurements not only outperforms the MultiCal algorithm in the presence of measurement noise, but also accurately estimates the uncertainty of its results.

The multiline TRL algorithm of [1] combines compactness and speed with an effective weighting and averaging strategy based on Gauss-Markov estimates. The algorithm was optimized for on-wafer measurements, and has been incorporated into the convenient and popular MultiCal software package.

The iterative approaches of [2] and [3] offer alternative solutions to the multiline TRL problem based on a nonlinear least-squares solutions to the conventional VNA and six-port calibration problems, respectively. While the iterative approaches are slower and less compact than the algorithm of [1], they are designed for optimal performance in the presence of measurement noise.

Reference [4] extended the basic approach of [2] to a 16-term error model and developed error estimates. Reference [5] applied the nonlinear least-squares approach to nonlinear vector network analyzers.

We later adapted the nonlinear least-squares solution of [2] to the characterization of planar coupled transmission lines in [6-9]. In this case, the least-squares solution was obtained using the orthogonal distance regression algorithm implemented in ODRPACK [10]. The

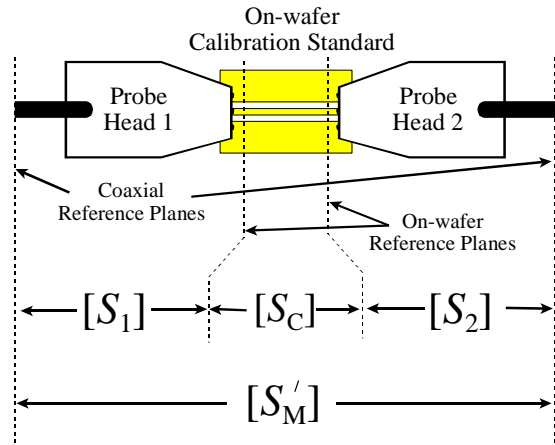


Fig. 1. The on-wafer calibration problem.

algorithms of [6-9] took advantage of the ability of ODRPACK to determine confidence intervals for the results directly from measurement data.

In this work, we adapt the calibration algorithm of [2] to the orthogonal distance regression algorithm of [10]. As in [2], the new algorithm finds an optimal solution to the multiline TRL on-wafer calibration problem in the presence of random measurement errors. In addition, the new algorithm determines confidence intervals for its results.

In this paper, we demonstrate that this new adaptation of [2] outperforms the multiline TRL calibration algorithm of [1] in the presence of random measurement errors. We also verify the accuracy of its uncertainty estimates.

II. THE CALIBRATION PROBLEM

Figure 1 shows a diagram of the two-tier on-wafer measurement problem that we address with the new calibration algorithm. The matrices $[S_1]$ and $[S_2]$ contain the scattering parameters of two microwave ground-signal-ground probe heads to be characterized. The matrix $[S_C]$ contains the scattering parameters of the on-wafer calibration standard contacted by the probes. The elements

³ MultiCal may be obtained at www.boulder.nist.gov/micro

* US government publication, not subject to copyright.

of $[S_M']$ are the scattering parameters of the cascade of the two probe heads with scattering-parameter matrices $[S_1]$ and $[S_2]$ and the calibration standard with scattering-parameter matrix $[S_C]$ measured by a network analyzer at the coaxial reference plane indicated in the figure. Here the prime indicates that $[S_M']$ is a measured, rather than a calculated, quantity. The objective of the calibration is to determine the scattering-parameter matrices $[S_1]$ and $[S_2]$ of two probe heads from measurements $[S_M']$ of the probes and on-wafer calibration standards.

In the multiline TRL calibration, the on-wafer standards consist of a short “thru” line, a set of additional on-wafer transmission lines of different lengths, and a symmetric “reflect” [11]. In other on-wafer calibration methods, the lines and/or reflect may be replaced by a variety of previously characterized terminations or other on-wafer calibration standards.

III. THE CALIBRATION ALGORITHM

The orthogonal distance regression algorithm implemented in ODRPACK [10] finds an optimal solution for β of the n equations

$$y_i = f_i(x_i + \delta_i, \beta) - \varepsilon_i, \quad (1)$$

where the subscript i corresponds to the i^{th} of the n “observations.” The f_i are functions relating the measurements y_i to the unknown vector β and the explanatory variables x_i . The ε_i and δ_i are the errors we wish to minimize in y_i and x_i .

To solve the calibration problem of Fig. 1, we set elements of the measurement vectors y_i to the real and imaginary parts of the elements of the measured scattering-parameter matrices $[S_M']$ of the two probes and calibration standard. The vector β contains the unknowns we wish to determine: we assigned elements of β to the real and imaginary parts of the elements of the scattering-parameter matrices $[S_1]$ and $[S_2]$ of the probe heads and, when appropriate, the propagation constant γ of the on-wafer transmission-line standards and the unknown reflection coefficients of any symmetric on-wafer reflect standards.

The vectors x_i contain sets of “explanatory” variables for each observation. We use them to add previously characterized standards to the calibration, setting elements of the x_i to the real and imaginary parts of the elements of the scattering-parameter matrix $[S_C]$ of the calibration standard. This strategy not only allows the algorithm to accommodate imperfectly characterized calibration standards, but it allows it to be applied to a broad range of calibration problems, including TRL, open-short-load-thru (OSLT) and line-reflect-match (LRM) calibrations. However, since the TRL calibration does not rely on

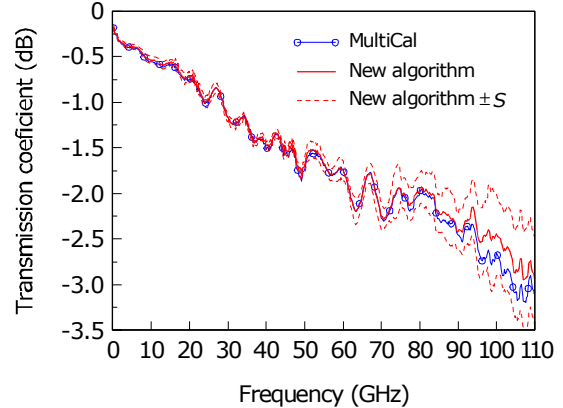


Fig. 2. Qualitative measurement comparison.

previously characterized calibration standards, there is no need for the explanatory variables x_i or their associated errors δ_i and weights w_δ for that special case.

The optimal solution for β is found by minimizing

$$\sum_{i=1}^n (\varepsilon_i^T w_{\varepsilon_i} \varepsilon_i + \delta_i^T w_{\delta_i} \delta_i), \quad (2)$$

subject to the constraints in (1), where the matrices w_ε and w_δ are weights. In our implementation of the on-wafer calibration algorithm, we set w_ε and w_δ equal to estimates of the inverse of the covariance matrices of errors in y_i and x_i supplied by the user, which improves the estimate of the unknowns in the vector β obtained with uniform weighting [10].

IV. QUALITATIVE MEASUREMENT COMPARISON

We compared the performance of our new calibration algorithm based on orthogonal distance regression to the algorithm of [1] implemented in MultiCal. Figure 2 compares the magnitude of the transmission coefficient of the first probe head estimated by the two algorithms for one of our typical on-wafer calibrations. The figure shows that the MultiCal estimates are close to the new calibration algorithm’s estimates and, in fact, usually lie well within the standard uncertainty s as estimated by the new algorithm. We obtained similar results for both the magnitudes and phases of all of the scattering parameters of the probe head.

V. QUANTITATIVE MEASUREMENT COMPARISON

We developed a simulator to examine more closely the performance of the two algorithms. The simulator began with the measured scattering parameters $[S_1]$ and $[S_2]$ of the two probe-heads and propagation constant of the lines,

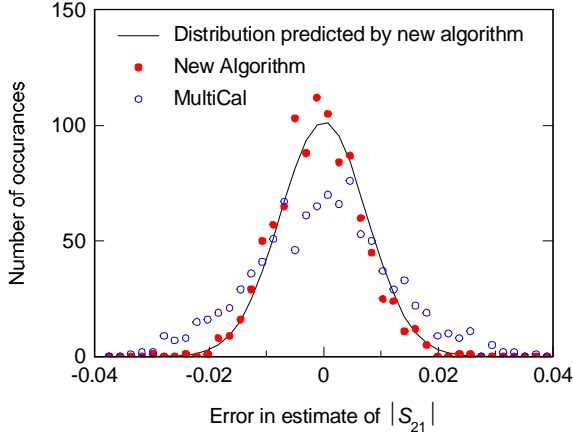


Fig. 3. Distribution of the error in the estimates of $|S_{21}|$ of the two algorithms with $\sigma_R = \dot{\sigma}_R = 0.01$ and $\sigma_T = \dot{\sigma}_T = 0.03$.

as determined from the experiment described in the last section. We first used the simulator to generate the exact values of $[S_M]$ corresponding to each of the standards used in the calibration, and verified that the two algorithms did solve for $[S_1]$ and $[S_2]$ exactly in the absence of measurement errors.

We then used the simulator to add Gaussian noise with standard deviation σ_R to the real and imaginary parts of the reflection coefficients and with standard deviation σ_T to the real and imaginary parts of the transmission coefficients in $[S_M]$, creating 1000 “noisy” measurements $[S_{Mk}]$. Finally, we used MultiCal and the new algorithm to estimate the scattering parameters $[S_{1k}]$ and $[S_{2k}]$ of the probes from the 1000 noisy measurements $[S_{Mk}]$. For each simulation we set the diagonal elements of the weights w_e to $\dot{\sigma}_R^{-2}$ or $\dot{\sigma}_T^{-2}$, as appropriate.

Figure 3 shows the distribution of the magnitude errors $||[S_{1k}]_{21}| - |[S_1]_{21}||$ in the estimates of the first error box’s transmission coefficient we obtained with the two algorithms. The figure shows that the new algorithm’s error distribution is more concentrated around 0 than MultiCal’s error distribution. This shows that the new algorithm does a better job of estimating the true value of $|S_{21}|$ than MultiCal does.

The solid line in the figure shows the estimated error distribution generated from the mean of the 1000 uncertainties predicted by the new algorithm. The two distributions show good agreement, giving us greater confidence in the ability of the new algorithm to estimate its own uncertainty.

Tables 1-3 investigate the linear errors of the two algorithms and will quantify these observations for our results at 50 GHz: we obtained similar results at 110 GHz.

A. Bias in the Algorithms

Let Δz represent the differences of estimates of z from the true value of z . The t statistic $t = \overline{\Delta z} / s_z$ is the ratio of the mean of Δz , which we write as $\overline{\Delta z}$, and the standard uncertainty s_z of $\overline{\Delta z}$. Large values of t indicate significant bias in the estimates of z .

We compiled t statistics to look for bias in MultiCal and the new algorithm in Table 1, where z corresponded to estimates of elements of $[S_1]$ generated by the algorithms. Here Δz corresponds to the difference between (a) the element of $[S_{1k}]$ listed in the first column of the table determined from the noisy measurements $[S_{Mk}]$ and (b) the true value of the element in $[S_1]$, $\overline{\Delta z}$ is the mean of the 1000 Δz , and s_z is the standard uncertainty of $\overline{\Delta z}$. From the table we conclude that neither algorithm adds a statistically significant bias into its estimates in the presence of Gaussian noise.¹

Table 1.

The t statistic for the algorithms. ($\sigma_R = \dot{\sigma}_R = \sigma_T = \dot{\sigma}_T = 0.01$)

z ($\in [S_1]$)	MultiCal	New Algorithm
$\text{Re}(S_{11})$	0.4	0.7
$\text{Re}(S_{22})$	0.02	0.02
$ S_{21} $	1.3	0.8
Angle S_{21}	0.2	-0.3

B. Variance of the Algorithms

To further explore the performance of the two algorithms, we estimated s_{MC} , the uncertainty in the MultiCal estimates, and s_{NEW} , the uncertainty in the new algorithm’s estimates. We estimated s_{MC} and s_{NEW} from the standard deviation of the differences of the 1000 noisy estimates $[S_{1k}]$ and the true values $[S_1]$. We tabulated our estimates of s_{MC} and s_{NEW} , as well as our estimate of s_{MC}/s_{NEW} , in Table 2.

We also list the 95% lower confidence bound B_L for the ratio based on our estimate of s_{MC}/s_{NEW} in the last column of Table 2, calculated from the F distribution with 999 and 999 degrees of freedom using $B_L \equiv s_{MC} / (s_{NEW} \sqrt{F_{0.95}})$. There is a 95% certainty that the actual value of the ratio is greater than B_L .

Table 2 shows that the uncertainty s_{MC} in the MultiCal estimates is consistently greater than the uncertainty in the estimates determined by the new algorithm. Furthermore, the table shows that the new algorithm outperforms MultiCal even when it is not supplied with accurate

¹ From the t distribution with 999 degrees of freedom we see that a value of $|t| > 1.96$ is required to conclude with 95% certainty that the estimates have a statistically significant bias.

estimates $\hat{\sigma}_T$ of the noise in the measurements. Finally, the table indicates that MultiCal has particular difficulty in the presence of noise in transmission-coefficient measurements.

Table 2.
Uncertainty of the two algorithms. ($\sigma_R = \hat{\sigma}_R = 0.01$)

z ($\in [S_{11}]$)	σ_T	$\hat{\sigma}_T$	s_{MC} ($\times 10^{-3}$)	s_{NEW} ($\times 10^{-3}$)	s_{MC}/s_{NEW}	B_L
Re(S_{11})	0.01	0.01	4.96	4.74	1.05	0.997
S_{21}	0.01	0.01	5.50	4.40	1.25	1.19
Re(S_{11})	0.03	0.01	6.36	5.13	1.24	1.18
S_{21}	0.03	0.01	11.8	7.43	1.58	1.50
Re(S_{11})	0.03	0.03	6.36	5.06	1.26	1.20
S_{21}	0.03	0.03	11.8	7.32	1.61	1.53

C. Uncertainty Estimate Generated by the New Algorithm

The new algorithm uses the residual deviations of the measurements from the electrical calibration model to estimate the uncertainties in its own results.² Table 3 investigates the accuracy of the standard-uncertainty estimates s generated by the new algorithm. The table compares the actual standard deviation σ_{ACTUAL} of the quantities in the first column of the table to the mean \bar{s} of the standard uncertainty estimates s generated by the new algorithm. The nearly identical values of σ_{ACTUAL} and \bar{s} indicate that, on average, the new algorithm accurately estimates the uncertainty in its results due to random measurement noise.

The quantity $u(s)/\bar{s}$ in the last column of Table 3 represents the ratio of the standard deviation $u(s)$ of the estimates s to their mean value \bar{s} . The small values of $u(s)/\bar{s}$ indicate that the new algorithm estimates the uncertainty of its results with reasonable consistency.

V. CONCLUSION

We compared a new vector-network-analyzer multiline TRL calibration algorithm based on the iterative approach of [2] with the orthogonal distance regression method of [9] to the TRL algorithm of [1] implemented in MultiCal. We showed that the new calibration algorithm outperforms the MultiCal algorithm in the presence of random measurement error and estimates the uncertainty of its results with reasonable accuracy.

² MultiCal estimates only the relative uncertainty in its results as a function of frequency.

Table 3.
Accuracy of s . ($\sigma_R = \hat{\sigma}_R = \sigma_T = \hat{\sigma}_T = 0.01$)

z ($\in [S_{11}]$)	σ_{ACTUAL}	\bar{s}	$u(s)/\bar{s}$
Re(S_{11})	0.0047	0.0046	0.12
Re(S_{22})	0.0055	0.0054	0.12
S_{21}	0.0044	0.0044	0.12
Angle S_{21}	0.324	0.297	0.30

SOFTWARE

Software implementing this method can be downloaded at <http://www.boulder.nist.gov/dylan/>.

REFERENCES

- [1] R.B. Marks, "A multiline method of network analyzer calibration," *IEEE Trans. Microwave Theory Tech.*, vol. MTT-39, no. 7, pp. 1205-1215, July 1991.
- [2] D.F. Williams, "De-embedding and unterminating microwave test fixtures with nonlinear least squares," *IEEE Trans. Microwave Theory Tech.*, vol. 38, no. 6, pp. 787-791, June 1990.
- [3] R.M. Judish and G.F. Engen, "On-line accuracy assessment for the dual six-port ANA: statistical methods for random errors," *IEEE Trans. Inst. Meas.*, vol. IM-36, no. 2, pp. 507-513, June 1987.
- [3] H. Van hamme and M. Vanden Bossche, "Flexible vector network analyzer calibration with accuracy bounds using an 8-term or a 16-term error correction model," *IEEE Trans. Microwave Theory and Tech.*, vol. 42, no. 6, pp. 976-987, June 1994.
- [4] W. Van Moer and Y. Rolain, "Calibration of a wideband IF nonlinear vectorial network analyzer," 53rd ARFTG Conf. Dig., pp. 98-103, June 1999.
- [5] D. F. Williams, "Calibration in Multiconductor Transmission Lines," 48th ARFTG Conf. Dig. (Orlando, FL), pp. 46-53, Dec. 4-6, 1996.
- [6] D.F. Williams, "Multiconductor transmission line characterization," *IEEE Trans. Components, Packaging, and Manufacturing Technol.-Part B*, vol. 20, no. 2, pp. 129-132, May 1997.
- [7] D.F. Williams, J.E. Rogers, and C.L. Holloway, "Multiconductor transmission line characterization: representations, approximations, and accuracy," *IEEE Trans. Microwave Theory Tech.*, vol. 47, no. 4, pp. 403-409, April 1999.
- [8] U. Arz, D.F. Williams, D.K. Walker, and H. Grabinski, "Asymmetric coupled CMOS lines: an experimental study," *IEEE Trans. Microwave Theory Tech.*, vol. 48, no. 12, pp. 2409-2414, Dec. 2000.
- [9] P.T. Boggs, R.H. Byrd, J.E. Rogers, and R.B. Schnabel, "User's reference guide for ODRPACK version 2.01 software for weighted orthogonal distance regression," *Nat. Inst. Stand. Technol. Internal Report*, NISTIR 92-4834, June 1992.
- [10] R.B. Marks and D.F. Williams, "A general waveguide circuit theory," *J. Res. Nat. Inst. Stand. Technol.*, vol. 97, pp. 533-562, 1992.